

2022-08-01

## Optimization Of Quantum Circuits Using Spin Bus Multiqubit Gates For Quantum Dots

Miguel Gonzalo Rodriguez  
*University of Texas at El Paso*

Follow this and additional works at: [https://scholarworks.utep.edu/open\\_etd](https://scholarworks.utep.edu/open_etd)



Part of the [Quantum Physics Commons](#)

---

### Recommended Citation

Rodriguez, Miguel Gonzalo, "Optimization Of Quantum Circuits Using Spin Bus Multiqubit Gates For Quantum Dots" (2022). *Open Access Theses & Dissertations*. 3625.  
[https://scholarworks.utep.edu/open\\_etd/3625](https://scholarworks.utep.edu/open_etd/3625)

This is brought to you for free and open access by ScholarWorks@UTEP. It has been accepted for inclusion in Open Access Theses & Dissertations by an authorized administrator of ScholarWorks@UTEP. For more information, please contact [lweber@utep.edu](mailto:lweber@utep.edu).

OPTIMIZATION OF QUANTUM CIRCUITS USING SPIN BUS MULTIQUBIT  
GATES FOR QUANTUM DOTS

MIGUEL GONZALO RODRIGUEZ

Master's Program in Physics

APPROVED:

---

Yun-Pil Shim, Ph.D., Chair

---

Mark R. Pederson, Ph.D.

---

Vladik Kreinovich, Ph.D.

---

Stephen L. Crites, Jr., Ph.D.  
Dean of the Graduate School

©Copyright

by

Miguel Rodriguez

2022

*to my*  
*ENTIRE FAMILY*  
*with love*

OPTIMIZATION OF QUANTUM CIRCUITS USING SPIN BUS MULTIQUBIT  
GATES FOR QUANTUM DOTS

by

MIGUEL GONZALO RODRIGUEZ, B.S.

THESIS

Presented to the Faculty of the Graduate School of

The University of Texas at El Paso

in Partial Fulfillment

of the Requirements

for the Degree of

MASTER OF SCIENCE

DEPARTMENT OF PHYSICS

THE UNIVERSITY OF TEXAS AT EL PASO

August 2022

# Acknowledgements

I want to express my deep-felt gratitude to my advisor, Dr. Yun-Pil Shim of the Physical Science Department at The University of Texas at El Paso, for his advice, encouragement, enduring patience, and constant support. In addition, I'd like to express my gratitude to the physics faculty for allowing me to complete my graduate studies and put my scientific abilities to the test. Without my committee members, Dr. Pedersen and Dr. Kreinovich, I would not be able to present my thesis for defense, and I am thankful to them for their willingness to do so.

NOTE: This thesis was submitted to my Supervising Committee on July 18, 2022.

# Abstract

Chapter 1 contains a short preamble with some of the most important notions of quantum computing, the fundamental components of which are critical for understanding the development of new circuits. Chapter 2 demonstrates how the optimum decomposition of some of the most often used circuits in quantum computing is that decomposition in actual physical processes that we may employ in electron-spin quantum dot-based quantum computers. This decomposition for devices based on the Loss and DiVincenzo scheme illustrates that the number of interaction operations between qubits rises with distance, causing the steps required to achieve the goal state to increase.

Chapter 3 demonstrates a different architecture that can be created using the same concepts for quantum computing based on quantum dots, allowing interaction operations between qubits to be performed more efficiently using a spin bus without increasing the number of steps with the number of qubits.

Chapter 4 demonstrates how we can implement this architecture based on the spin bus in interleaving circuits and important circuits such as quantum error correction, using numerical optimization methods to obtain the circuit with the fewest number of operations that approximates the target state as closely as possible. The spin bus technique is substantially more efficient for long-distance interactions between the circuit's qubits.

# Table of Contents

	<b>Page</b>
Acknowledgements . . . . .	v
Abstract . . . . .	vi
Table of Contents . . . . .	vii
List of Tables . . . . .	ix
List of Figures . . . . .	x
<b>Chapter</b>	
1 Introduction . . . . .	1
1.1 Qubit . . . . .	1
1.1.1 Spin Qubit . . . . .	1
1.1.2 Quantum Mechanical Properties for Qubits . . . . .	2
1.1.3 Qubit State . . . . .	3
1.1.4 Bloch Sphere Representation . . . . .	3
1.1.5 Phase . . . . .	4
1.2 Single-Qubit Operation . . . . .	5
1.2.1 Pauli Operators . . . . .	6
1.2.2 Single-Qubit Rotations . . . . .	8
1.2.3 Hadamard Gate . . . . .	10
1.3 Two-Qubit Operations . . . . .	10
1.3.1 Exchange Interaction . . . . .	11
1.3.2 Heisenberg exchange interaction . . . . .	12
1.3.3 Controlled gates . . . . .	13
1.4 Quantum Circuits . . . . .	13
2 Optimization of Quantum Circuits Using Exchange Gate Steps . . . . .	15
2.1 CNOT . . . . .	15

- 2.2 Bell’s State . . . . . 16
- 2.3 GHZ State . . . . . 17
- 2.4 Quantum Error Correcting Code . . . . . 17
  - 2.4.1 Quantum Error Correcting Code for Three Qubits . . . . . 18
  - 2.4.2 Quantum Error Correcting Code for Five Qubits . . . . . 20
  - 2.4.3 Quantum Error Correcting Code for Seven Qubits . . . . . 21
- 3 Spin Bus . . . . . 22
  - 3.1 Spin Bus Architecture . . . . . 22
  - 3.2 Build Multiqubit Bus Gates . . . . . 25
- 4 Optimize Quantum Circuits Using Spin Bus Multiqubit Gate . . . . . 28
  - 4.1 Optimization of Quantum Circuits Using Spin Bus . . . . . 28
  - 4.2 Optimization of Error Correcting Codes Using Spin Bus Gates . . . . . 30
  - 4.3 Comparison . . . . . 31
- 5 Conclusion . . . . . 34
- References . . . . . 35
- Curriculum Vitae . . . . . 38

# List of Tables

4.1	Comparison of the number of multiqubit gates and number of total steps necessary for the construction of the CNOT gate with 1,2,4 and n qubits of distance. . . . .	32
4.2	Comparison of number of multiqubit gates and number of total steps needed to create circuits to obtain entangled states between qubits. . . . .	32
4.3	Comparison of number of multiqubit gates and number of total steps needed to create QECC for 3,5 and 7 qubits. . . . .	33

# List of Figures

1.1	Example of Bloch sphere representation. Graph generated by: [8]. . . . .	4
1.2	Pauli rotations of the Bloch Sphere. Graph generated by: [8] . . . . .	6
3.1	”The spin bus is a chain of electronic spins ( $\bullet$ ) with strong, static couplings (heavy lines). External qubits ( $\circ$ ) can be coupled to the bus at any node (light lines). Effective long-range interactions allow for communication between sectors dedicated to rotation, readout or memory, which may benefit from isolation.” [25] . . . . .	23
3.2	Additional local couplings enable parallel interactions, in addition to bus-mediated interactions [25]. . . . .	24
3.3	Within the ground state manifold, the bus acts as a simple spin-1/2 qubit, except for its plurality of qubit couplings. . . . .	25
3.4	With at special times, the unitary operator becomes the bus gates angles only the qubits, not the bus pseudospin . . . . .	26

# Chapter 1

## Introduction

### 1.1 Qubit

A qubit can be any two-level quantum system. The single electron, which has two spin states ( $S_z = -\hbar/2$  and  $S_z = \hbar/2$ ), is the classic contender for such a system [1, 2]. The physical position of the electron es en si un spin qubit within a single semiconductor quantum dot and qubit manipulation is limited to the rotation of the electron spin [1].

#### 1.1.1 Spin Qubit

A qubit can also be the actual location of an electron within a double quantum dot. In this example, the electron occupying the left or right quantum dot is the two-qubit state and spin [1, 2]. A key concept in understanding quantum computer realization is the notion of quantum noise (sometimes called decoherence). “It is generally desirable to have some aspect of symmetry dictate the finiteness of the state space to minimize decoherence.” [3] A spin-1/2 particle, for example, resides in a Hilbert space spanned by the  $|S+\rangle$  and  $|S-\rangle$  states; the spin state cannot be anything other than this two-dimensional space, making it a nearly ideal quantum bit when well isolated [3]. Then, one of the essential prerequisites for creating quantum logic devices is a high level of quantum coherence. Coherence is lost when a qubit interacts with other quantum degrees of freedom in its surroundings and becomes entangled [4]. Predicting the coherence time of the electron spin states of a device functioning with spin quantum dots is difficult since all of the system’s quantum degrees of freedom must be addressed [3, 4].

### 1.1.2 Quantum Mechanical Properties for Qubits

There are specific quantum mechanical properties to building a qubit. One of these is that the qubit can be in any proportion of both states at simultaneously. This property is the *superposition* [2, 5, 3]. The qubit is in a coherent superposition 0 and 1 long as it is unmeasured. There are two potential outcomes for measuring a qubit: 0 and 1, much like a bit. Furthermore, although measuring a conventional bit does not damage its state, measuring a qubit destroys its coherence and irreversibly disturbs the superposition state, causing it to collapse into one of two states. One bit can be entirely encoded in one qubit, and a qubit, on the other hand, can store more information. [5].

Other property is *quantum interference*, this property affects the chance of a qubit collapsing in one direction. Quantum interference modifies the state of a qubit to impact the likelihood of a specific outcome during measurement. The power of quantum computing shines most in this probabilistic state [5, 3]. Four classical bits, for example, can simultaneously be in one of two to the power of four different configurations. On the other hand, four qubits in superposition can be in all 16 designs simultaneously. With each additional qubit, this number grows exponentially, and twenty of them can currently store a million values in parallel [5].

*Entanglement* is a peculiar and unintuitive property in qubits that can have a close connection that makes each of the qubits react to a change in the other's state instantaneously, no matter how far they are apart. When measuring just one entangled qubit, we can directly deduce its partners' properties without looking [5, 3].

A standard logic gate gets a simple set of inputs and produces one actual output. A quantum gate manipulates information of superpositions, rotates probabilities, and has another superposition. So a quantum computer sets up some qubits, applies quantum gates to entangle them and use possibilities, then finally measures the outcome, collapsing superpositions to an actual sequence of 0s and 1s [5, 3]. We get the many possible calculations with our setup, all done simultaneously.

### 1.1.3 Qubit State

A classical bit, or basic unit of classical information, can only have two mutually incompatible values, such as 1 or 0. Through a complex-valued superposition of the two entire states, it is a quantum analog, and the qubit can span the continuous space between the two values:

$$|\Psi\rangle = a|0\rangle + b|1\rangle \quad (1.1)$$

where  $a$  and  $b$  are complex variables. As a result in equation (1.1), the qubit can store an unlimited quantity of data. Processing such data could result in extreme parallelism, as a single operation could simultaneously modify an infinite data collection. However, because a measurement collapses the superposition to one of the exclusive values, leaving no trace of the superposition, the resulting information is not directly accessible. Repeated trials demonstrate the existence of the superposition through a statistical distribution of the outcomes, which reflects the continuous value of the superposition coefficient [6, 7].

### 1.1.4 Bloch Sphere Representation

We will start with the action of a quantum gate on a single quantum bit. A single classical bit is relatively dull, either zero or one. On the other hand, a quantum bit is a much richer object that can exist in a quantum superposition of zero and one. “This representation is a point on the surface of a three-dimensional ball known as a Bloch sphere” [3, 7]. A 1-qubit gate’s action is to rotate the point on this sphere around some axis.

$$|qubit\rangle = |\psi\rangle = \cos\left(\frac{1}{2}\theta\right)|0\rangle + e^{i\phi}\sin\left(\frac{1}{2}\theta\right)|1\rangle \quad (1.2)$$

$$\vec{n} = (\sin\theta\cos\phi, \sin\theta\sin\phi, \cos\theta) \quad (1.3)$$

In the Figure 1.1, we can see the representation of the 1-qubit’s state with a red line. Equation 1.2 represents the state of a single qubit and parameterized for two angles  $\theta$  and  $\phi$ . The parameters  $\theta$  and  $\phi$  can be interpreted as spherical coordinates of a point on the surface of a unit sphere, where  $\theta$  is the colatitude for the z-axis and  $\phi$  the longitude to the

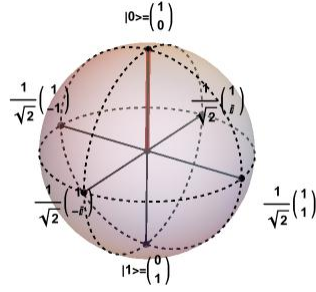


Figure 1.1: Example of Bloch sphere representation. Graph generated by: [8].

x-axis,  $0 \leq \theta \leq \pi$  and  $0 \leq \phi \leq 2\pi$ . In cartesian coordinates, the point on the 3-dimensional unit sphere is given by the equation (1.3).

### 1.1.5 Phase

In quantum physics, the term phase has various different interpretations depending on the context. For instance, consider the state  $e^{i\theta}|\psi\rangle$ , where  $|\psi\rangle$  is a state vector, and  $\theta$  is a real number. We argue that the state  $e^{i\theta}|\psi\rangle$  is equal to  $|\psi\rangle$ , up to the *global phase factor*  $e^{i\theta}$  [3, 7, 9, 10]. It is worth noting that the measurement statistics anticipated for these two situations are identical. [3]. To demonstrate this, suppose  $M_m$  is a measurement operator associated with some quantum measurement, observe that the respective probability for outcome  $m$  occurring are  $\langle\psi|M_m^\dagger M_m|\psi\rangle$  and  $\langle\psi|M_m^\dagger M_m|\psi\rangle = \langle\psi|e^{-i\theta}M_m^\dagger M_me^{i\theta}|\psi\rangle$ . As a result, from an observable standpoint, these two states are identical. As a result, we can disregard global phase effects as unrelated to the observed physical system features. [3]. There is another kind of phase known as the *relative phase*, which has quite a different meaning. Consider the states

$$\frac{|0\rangle + |1\rangle}{\sqrt{2}} \quad \text{and} \quad \frac{|0\rangle - |1\rangle}{\sqrt{2}} \tag{1.4}$$

In the first state the amplitude of  $|1\rangle$  is  $\frac{1}{\sqrt{2}}$ . For the second state the amplitude is  $-\frac{1}{\sqrt{2}}$ . In each case the magnitude of the amplitudes is the same, but they differ in sign. More

generally, we say that two amplitudes,  $a$  and  $b$ , differ by a relative phase if there is a real  $\theta$  such that  $a = e^{i\theta}b$ . More generally still, two states are said to differ by a relative phase in some basis if each of the amplitudes in that basis is related by such a phase factor. For example, the two states displayed above are the same up to a relative phase shift because the  $|0\rangle$  amplitudes are identical (a relative phase factor of 1), and the  $|1\rangle$  amplitudes differ only by a relative phase factor of  $-1$  [3]. The difference between relative phase factors and global phase factors is that for relative phase the phase factors may vary from amplitude to amplitude. This makes the relative phase a basis-dependent concept unlike global phase [3]. As a result, states which differ only by relative phases in some basis give rise to physically observable differences in measurement statistics, and it is not possible to regard these states as physically equivalent, as we do with states differing by a global phase factor [3]. We get the following from equation (1.1):

$$|\Psi\rangle = a|0\rangle + b|1\rangle \quad \text{where } |a| + |b| = 1 ; a, b \in \mathbb{C} \tag{1.5}$$

We can re-write the equation (1.1) as follows:

$$|\psi\rangle = e^{i\zeta}(\cos(\frac{1}{2}\theta)|0\rangle + e^{i\phi} \sin(\frac{1}{2}\theta)|1\rangle) \tag{1.6}$$

where  $\zeta, \theta$  and  $\phi$  are real numbers, and the coefficients  $a$  and  $b$  are complex numbers. The phase factor  $e^{i\zeta}$  has no physical effect and can thus be ignored. It is simply a byproduct of mathematical representation [3]. (If we use a density matrix representation, the phase factor vanishes entirely.)

$$|\psi\rangle \simeq \cos(\frac{1}{2}\theta)|0\rangle + e^{i\phi} \sin(\frac{1}{2}\theta)|1\rangle \tag{1.7}$$

We will use  $\simeq$  to indicate that two states (or gates) are equal to a global phase factor.

## 1.2 Single-Qubit Operation

A set of operations can be described that transforms the collective state of a quantum bus, an enumerated collection of qubits, without collapsing the system's quantum state. The

unitary and reversible operators fulfill this requirement. The quantum operator formalism has borrowed the linear algebra language due to a system's superposition state as a complex vector. A quantum operator is often represented as a matrix since it changes one vector into another.

$$|\Psi\rangle = M|\Phi\rangle \tag{1.8}$$

where  $|\Psi\rangle$  and  $|\Phi\rangle$  are vectors, and matrix elements of  $M$  are obtained through an  $|e_i\rangle$  basis projection:  $M_{ij} = \langle e_i|e_j\rangle$ . A unitary operator on a vector space is a linear operator that is length-preserving. A reversible operator is bijective, i.e. has a well-defined inverse. These concepts are well understood in linear algebra, have been translated to constraints on matrix properties, and time dependent evolution of an isolated quantum system has been demonstrated to obey such rules [3, 7].

### 1.2.1 Pauli Operators

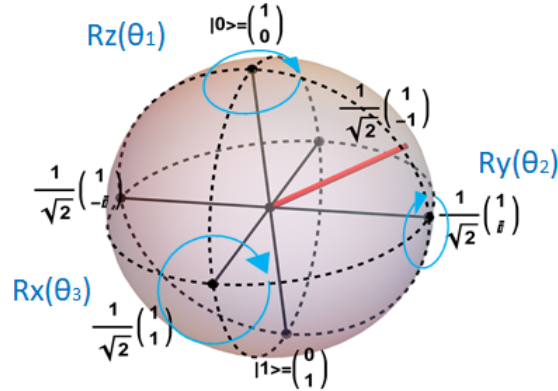


Figure 1.2: Pauli rotations of the Bloch Sphere. Graph generated by: [8]

The four gates represented by the Pauli operators,  $I, X, Y,$  and  $Z,$  are the most basic 1-qubit gates. These operators are also sometimes written as  $\sigma_x, \sigma_y,$  or  $\sigma_z$  or with the index

I so that  $\sigma_0 = I, \sigma_1 = X, \sigma_2 = Y,$  and  $\sigma_3 = Z$ . The Pauli gates are all Hermitian,  $\sigma_i = \sigma_i^\dagger$  square to the identity  $\sigma_i^2 = I$ , and that the  $X, Y,$  and  $Z$  gates anti-commute with each other [3, 7].

Pauli-I gate (identity):

$$I = \begin{bmatrix} 1 & 0 \\ 0 & 1 \end{bmatrix} \tag{1.9}$$

— $\boxed{I}$ —

The trivial no-operation gate on 1-qubit, represented by the identity matrix. Acting on any arbitrary state, the gate leave the state unchanged.

Pauli-X gate (X-gate, bit flip):

$$X = \begin{bmatrix} 0 & 1 \\ 1 & 0 \end{bmatrix} \tag{1.10}$$

— $\boxed{X}$ —

The X-gate generates a half-turn in the Bloch sphere about the x axis.

Pauli-Y gate (Y-gate):

$$Y = \begin{bmatrix} 0 & -i \\ i & 0 \end{bmatrix} \tag{1.11}$$

— $\boxed{Y}$ —

The Pauli-Y gate generates a half-turn in the Bloch sphere about the by y-axis.

Pauli-Z gate (Z-gate, phase flip):

$$Z = \begin{bmatrix} 1 & 0 \\ 0 & -1 \end{bmatrix} \tag{1.12}$$

— $\boxed{Z}$ —

The Pauli-Z gate generates a half-turn in the Bloch sphere about the z axis.

### 1.2.2 Single-Qubit Rotations

A  $2 \times 2$  unitary matrix,  $U$ , will correspond to a maximally general 1-qubit gate. Given that  $U$  is unitary, the determinant's magnitude must be one, or  $|\det(U)| = 1$ . Any one of the values of  $\det(U)$ ,  $+1$ ,  $-1$ ,  $+i$ , or  $-i$  can satisfy this equation. It is claimed that  $U$  is "special unitary" if  $\det(U) = +1$  [11]. If not, finding a circuit for the special unitary matrix  $V$  suffices to create a circuit for the unitary matrix  $U$  because doing so requires adding a phase shift gate ( $Ph(\alpha)$  to the circuit for  $V$ ). Realizing this makes it simple to see.

$$U = e^{i\alpha} \begin{bmatrix} 1 & 0 \\ 0 & 1 \end{bmatrix} * V = Ph(\alpha) * V \quad (1.13)$$

As  $V$  is a  $2 \times 2$  special unitary matrix its rows and columns are orthonormal and, its elements, most generally, are complex numbers and  $\alpha$  is real. Hence,  $V$  must have the form:

$$V = \begin{bmatrix} a & -b^* \\ b & a^* \end{bmatrix} \quad (1.14)$$

where  $a$  and  $b$  are complex with  $|a|^2 + |b|^2 = 1$ . Given such a generic unitary, we would like to represent this gate using standard parameterized gates. A quantum computer requires a library of quantum gates to represent or approximate a general unit transformation. All single-qubit gates and almost any fixed two-qubit gate operation can be constructed using a general unitary transformation [3, 6, 10]. Then each rotation axis corresponds to a particular Cartesian axis (Figure 1.2) the elementary, single-qubit rotations in matrix form are:

$$R_z(\theta_1) = \begin{pmatrix} \exp(i\theta_1/2) & 0 \\ 0 & \exp(-i\theta_1/2) \end{pmatrix} \quad (1.15)$$

$$R_y(\theta_2) = \begin{pmatrix} \cos(\theta_2/2) & \sin(\theta_2/2) \\ -\sin(\theta_2/2) & \cos(\theta_2/2) \end{pmatrix} \quad (1.16)$$

$$R_x(\theta_3) = \begin{pmatrix} \cos(\theta_3/2) & i \sin(\theta_3/2) \\ i \sin(\theta_3/2) & \cos(\theta_3/2) \end{pmatrix} \quad (1.17)$$

In a previous subsection we talked about the equivalence of the surface of a three-dimensional unit sphere and the representation of the state of a qubit as a two-dimensional complex vector [7]. The correct mathematical term for this equivalence in linear algebra is called isomorphism [13]. The Bloch sphere isomorphism identifies a unit vector Equation 1.3:  $\vec{n} = (n_x, n_y, n_z)$ , with  $\sigma_n = n_x\sigma_x + n_y\sigma_y + n_z\sigma_z$ . Rotation by angle around the vector  $\vec{n}$  corresponds to the special unitary operator  $R_n(\theta) = e^{-i\sigma_n\theta/2}$ . It is from this identification that the decomposition of an arbitrary one-qubit gate arise [3, 13]:

**Theorem 1** *Suppose  $V$  is a 1-qubit special unitary gate. Then there exist real numbers  $\alpha, \beta$  and  $\gamma$  such that*

$$V = R_z(\alpha)R_y(\beta)R_z(\gamma) \quad (1.18)$$

Proof: Since  $U$  is unitary, the rows and columns of  $U$  are orthonormal, from which it follows that there exist real numbers  $\alpha, \beta, \gamma$  and  $\delta$  such that

$$V = \begin{pmatrix} e^{i(-\alpha/2-\gamma/2)} \cos \frac{\beta}{2} & -e^{i(-\alpha/2-\gamma/2)} \sin \frac{\beta}{2} \\ e^{i(\alpha/2-\gamma/2)} \sin \frac{\beta}{2} & e^{i(\alpha/2+\gamma/2)} \cos \frac{\beta}{2} \end{pmatrix} \quad (1.19)$$

Equation (1.20) now follows immediately from the definition of the rotation matrices and matrix multiplication.

**Theorem 2** *Suppose  $U$  is a 1-qubit unitary gate. Then there exist real numbers  $\alpha, \beta, \gamma$  and  $\delta$  such that*

$$U = e^{i\delta} R_z(\alpha)R_y(\beta)R_z(\gamma) \quad (1.20)$$

Proof: Since  $U$  is unitary, the rows and columns of  $U$  are orthonormal, from which it follows that there exist real numbers  $\alpha, \beta, \gamma$  and  $\delta$  such that

$$U = \begin{pmatrix} e^{i(\delta-\alpha/2-\gamma/2)} \cos \frac{\beta}{2} & -e^{i(\delta-\alpha/2-\gamma/2)} \sin \frac{\beta}{2} \\ e^{i(\delta-\alpha/2-\gamma/2)} \sin \frac{\beta}{2} & e^{i(\delta-\alpha/2-\gamma/2)} \cos \frac{\beta}{2} \end{pmatrix} \quad (1.21)$$

This proof builds on the previous proof with the only extra of the multiplication of the phase term. Of course, the choice of y, z is arbitrary; one may take any pair of orthogonal vectors in place of y, z [3, 13].

### 1.2.3 Hadamard Gate

One of the most useful single-qubit gates, if not the most helpful, is the Hadamard gate, abbreviated  $H$ . The matrix defines the Hadamard gate:

$$H = \frac{1}{\sqrt{2}} \begin{pmatrix} 1 & 1 \\ 1 & -1 \end{pmatrix} \quad (1.22)$$

when the Hadamard gate  $H$  is applied to a computational basis state  $|x\rangle$ , it changes the input as follows:

$$H|x\rangle = \frac{1}{\sqrt{2}}(|0\rangle + (-1)^x|1\rangle) \quad (1.23)$$

The Hadamard gate's utility stems from the fact that by applying a different Hadamard gate to each of  $n$  qubits, each of which is initially in the state  $|0\rangle$ , we may produce an  $n$ -qubit superposition with  $2^n$  component eigenstates [11]. These eigenstates represent all bit strings that may be written with  $n$  bits. The significance of this capacity is sometimes overlooked. However, it is one of the essential quantum computing methods since it allows us to load exponentially many indices into a quantum computer using just several operations. If nature had been harsh and we had had to enter the different bit-strings separately, as in classical computing, quantum computing would have had significantly less potential for computational complexity advancements [11].

## 1.3 Two-Qubit Operations

Different Hamiltonians are related to different types of quantum computing gear. So, whereas obtaining a CNOT gate (for example) may be simple in one version, it may not be accessible in another. As a result, some of 2-qubit gates that are more “natural” in various forms of quantum computing hardware. There are guidelines for interchanging different types of 2-qubit gates so we can look at a quantum circuit defined using one gate family and map it into another, possibly easier to obtain, family. Physical interactions accessible in various forms of quantum computer hardware can give rise to many “natural” 2-qubit

gates such as  $\sqrt{SWAP}$ ,  $SWAP$ ,  $ISWAP$ ,  $CSIGN$ , and so on. These are often easier to produce than CNOT in the physical form in question and, if maximally entangling, provide no less efficient decompositions of arbitrary 2-qubit operations [11, 14].

$$\sqrt{SWAP} = \begin{pmatrix} 1 & 0 & 0 & 0 \\ 0 & \frac{1}{2} + \frac{i}{2} & \frac{1}{2} - \frac{i}{2} & 0 \\ 0 & \frac{1}{2} - \frac{i}{2} & \frac{1}{2} + \frac{i}{2} & 0 \\ 0 & 0 & 0 & 1 \end{pmatrix} \quad (1.24)$$

Because “spintronic quantum computing exploits the exchange interaction”,  $\sqrt{SWAP}$  and  $(SWAP)^\alpha$  inevitably emerge [11]. The exchange interaction will be further explored in the following section, as will the parameters on which the alpha value depends.

### 1.3.1 Exchange Interaction

A configurable exchange interaction generates two-qubit interactions in numerous generic solid-state quantum computing approaches [1, 2]. For example, a Heisenberg exchange between two-electron spin qubits results in a  $(SWAP)^\alpha$  gate [14], where the exponent alpha is controlled by modifying the strength and length of the Heisenberg exchange. It has been proposed that for solid-state computing, single-qubit rotations have also been prominent [10, 14]. In general, it is preferable to optimize quantum circuits in terms of the number of physical operations necessary, which for most solid-state quantum computation proposals means optimizing circuits in terms of the number of (SWAP) operations and single-qubit rotations [13, 14]. Heisenberg interaction Let’s first fix some notation, the four possible determined states of a pair of qubits are:  $|00\rangle, |10\rangle, |01\rangle$  and  $|11\rangle$ . The SWAP gate is defined as  $SWAP|\psi\rangle|\phi\rangle = |\phi\rangle|\psi\rangle$  when  $|\phi\rangle$  and  $|\psi\rangle$  are some two different random states for two-qubits, it can be written explicitly as:

$$SWAP = |00\rangle\langle 00| + |11\rangle\langle 11| + |01\rangle\langle 01| + |10\rangle\langle 10| \quad (1.25)$$

$$SWAP = \begin{pmatrix} 1 & 0 & 0 & 0 \\ 0 & 0 & 1 & 0 \\ 0 & 1 & 0 & 0 \\ 0 & 0 & 0 & 1 \end{pmatrix} \quad (1.26)$$

then  $(SWAP)^\alpha$ , can be written as:

$$(SWAP)^\alpha = |00\rangle\langle 00| + |11\rangle\langle 11| + (|01\rangle\langle 10| + |10\rangle\langle 01|)^\alpha \quad (1.27)$$

$$(SWAP)^\alpha = \begin{pmatrix} 1 & 0 & 0 & 0 \\ 0 & \frac{1 + e^{i\pi\alpha}}{2} & \frac{1 - e^{i\pi\alpha}}{2} & 0 \\ 0 & \frac{1 - e^{i\pi\alpha}}{2} & \frac{1 + e^{i\pi\alpha}}{2} & 0 \\ 0 & 0 & 0 & 1 \end{pmatrix} \quad (1.28)$$

### 1.3.2 Heisenberg exchange interaction

The Hamiltonian of the isotropic Heisenberg exchange interaction between electron spins  $\vec{S}_1$  and  $\vec{S}_2$  is:

$$H = J(t)\vec{S}_1 \cdot \vec{S}_2 \quad (1.29)$$

where  $\vec{S} = \{\sigma_x, \sigma_y, \sigma_z\}$  is a vector of Pauli matrices and  $J(t) = 4t_0^2(t)/u$ . Here  $u$  is the charging energy of a single dot [15]. The coupling constant  $J(t)$  can in principal be tuned for confined electrons [15]. The unitary operator generated by this Hamiltonian is:

$$U_{12} = \exp\left(-\frac{i}{\hbar}\vec{S}_1 \cdot \vec{S}_2 \int J(t)dt\right) \quad (1.30)$$

The unitary operator  $U_{12}$  can naturally implement the gate  $(SWAP)^\alpha$  where  $\alpha = \int J(t)dt/\hbar$  by modifying the integrated coupling  $\int J(t)dt/\hbar$ . Then the  $(SWAP)^\alpha$  gate is the two-qubit gate.

### 1.3.3 Controlled gates

“If A is true, then do B.” This controlled operation is precious in both conventional and quantum computing [3]. The prototypical controlled operation is the controlled-NOT, which we’ll often refer to as a quantum gate with two input qubits, known as the control qubit and target qubit, respectively [5]. In terms of the computational basis, the action of the CNOT is given by  $|c\rangle|t\rangle \rightarrow |c\rangle|t \oplus c\rangle$  where “ $\oplus$ ” represent addition modulo 2; that is, if the control qubit is set to  $|1\rangle$  then the target qubit is flipped, otherwise the target qubit is left alone. Thus, in the computational basis  $|control, target\rangle$  the matrix representation of is:

$$\begin{bmatrix} 1 & 0 & 0 & 0 \\ 0 & 1 & 0 & 0 \\ 0 & 0 & 0 & 1 \\ 0 & 0 & 1 & 0 \end{bmatrix} \tag{1.31}$$

This is the circuit representation for the controlled-NOT gate. The “.” in top line represents the control qubit and “ $\oplus$ ” in the bottom line represents the target qubit:



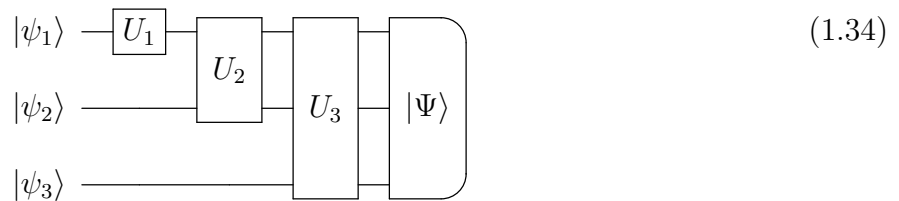
More generally, suppose  $U$  is an arbitrary single qubit unitary operation. A controlled- $U$  operation is a two qubit operation, again with a control and a target qubit [3]. If the control qubit is set then  $U$  is applied to the target qubit, otherwise the target qubit is left alone, that is,  $|c\rangle|t\rangle \rightarrow |c\rangle U^c|t\rangle$ . The controlled- $U$  operation is represented by the circuit shown:



## 1.4 Quantum Circuits

The definition of a quantum circuit is perfectly explained in the book by Philip Kaye et al. [7]: “In the quantum circuit model, we have logical qubits carried along ‘wires’,

and quantum gates that act on the qubits. A quantum gate acting on  $n$  qubits has the input qubits carried to it by  $n$  wires, and  $n$  other wires carry the output qubits away from the gate.” then quantum circuits are collections of quantum gates interconnected by quantum wires, described mathematically by a unitary transformation [3]. We must be aware that, unlike their classical equivalents, the input and output of a quantum circuit are not physically separated in a quantum computer; this convention allows us to explain the unitary transformation effect produced by the circuit more consistently [3].



An example of a quantum circuit is the Circuit 1.34 where there is first an initial state  $|\psi_i\rangle = |\psi_1\psi_2\psi_3\rangle$  that is used as the standard for the state of 0s but it is not mandatory in quantum systems. The gates are applied to it; in this case, we start with the unitary gate  $U_1$  that is applied only to the first qubit and only affects this state. In the next step in this example, the  $U_2$  gate is applied, where this is a multiqubit gate that can affect one or both qubits and even leave them entangled. In the next step, the  $U_3$  multiqubit gate is applied, affecting one, two, or even all three qubits. As a final step, the target state  $|\Psi\rangle = |\Psi_1\Psi_2\Psi_3\rangle$  is obtained, which collapses into a state of 0s and 1s when measured. The states of 0s and 1s are obtained with a certain probability of  $P$ ; this probability depends on the parameters  $P = |a_i|$  for collapses to state 0 and  $P = |b_i|$  for collapses to state 1 from  $|\Psi_i\rangle = a_i|0\rangle + b_i|1\rangle$  states of each qubit in the target state  $|\Psi\rangle$ .

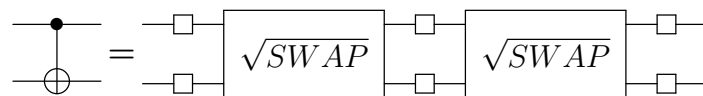
# Chapter 2

## Optimization of Quantum Circuits Using Exchange Gate Steps

This chapter explains the traditional method of creating some of the most commonly used circuits in quantum computing. These circuits are created using the most well-known architecture in which interaction between qubits can only be done between neighboring qubits, that is, pairs, which means increasing the number of qubits of the distance between two qubits that are desired to interact increases the number of interactions. Then the circuits are decomposed into real physical operations in quantum dot devices, such as rotations of 3 angles in 2 different orthogonal axes controlled by electromagnetic fields and exchange interactions:  $SWAP$  and  $\sqrt{SWAP}$  that appear naturally in electron-based quantum dot devices.

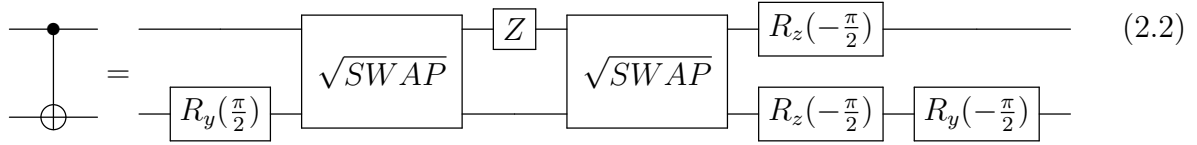
### 2.1 CNOT

To establish a CNOT gate between two adjacent qubits utilizing exchange interaction, two  $\sqrt{SWAP}$  gates must be used, as indicated in Circuit 2.1. The Circuit 2.2 is the most popular circuit for creating a CNOT gate from exchange interactions.

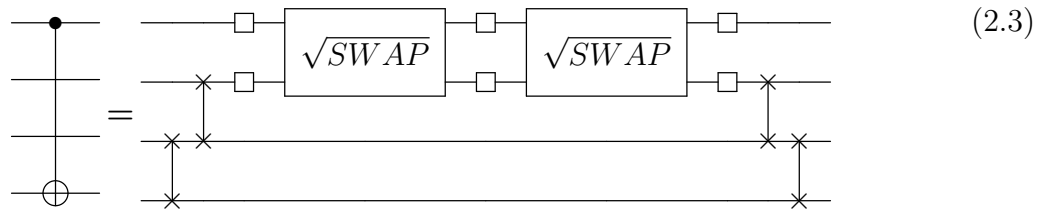


The diagram shows a quantum circuit with two horizontal lines representing qubits. On the left, a CNOT gate is shown with a control dot on the top line and a target circle on the bottom line. This is followed by an equals sign. To the right of the equals sign, the circuit consists of two  $\sqrt{SWAP}$  gates in series. Each  $\sqrt{SWAP}$  gate is represented by a rectangular box with the text  $\sqrt{SWAP}$  inside. The two qubit lines enter each box from the left and exit from the right. Small square markers are placed at the input and output points of each  $\sqrt{SWAP}$  gate. The entire equation is labeled (2.1) on the far right.

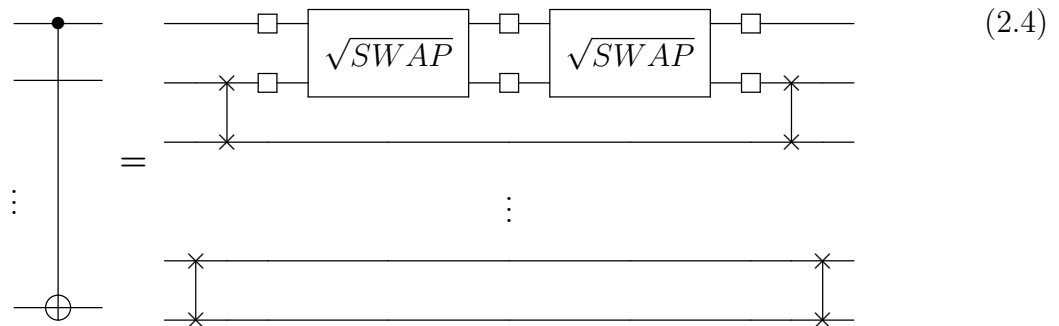
It needs 2 exchange gate steps (two  $\sqrt{SWAP}$ ) and 3 single qubits steps.



It is the most used way for obtaining a CNOT gate given the ability to achieve 1-qubit gates and  $\sqrt{SWAP}$  [3, 11]. Then 6 exchange interaction gate (2  $\sqrt{SWAP}$  and 4  $SWAP$ ) and three single qubit steps are used to create a CNOT gate with a distance of 3 qubits.



Then  $2n$  exchange interaction gate steps, which are 2  $\sqrt{SWAP}$  gates and  $(2n - 2)$   $SWAP$  gates, are used to create a CNOT gate n-qubits (more than 2 qubits) apart.



## 2.2 Bell's State

The Bell states or EPR pairs are specific quantum states of two qubits that represent "the simplest and maximal examples of quantum entanglement" [3].

$$|Bell\rangle = \frac{|00\rangle + |11\rangle}{\sqrt{2}} \quad (2.5)$$

To build a circuit that gives the Bell state Equation (2.5) as the target state, 2 exchange gate steps and 3 single qubit steps are required.

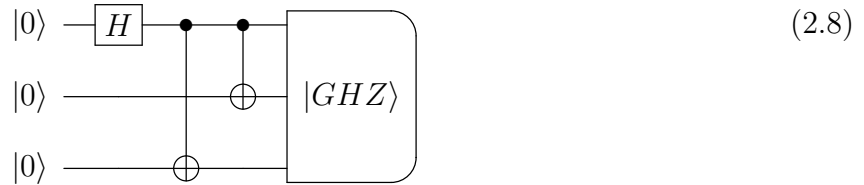


### 2.3 GHZ State

The GHZ (Greenberger–Horne–Zeilinger state) state is an entangled quantum state for 3 qubits and its state is described by equation (2.7) [3]

$$|GHZ\rangle = \frac{|000\rangle + |111\rangle}{\sqrt{2}} \tag{2.7}$$

So 6 exchange gate steps and six single qubit steps are required to build a circuit that provides the GHZ state as the target state.



### 2.4 Quantum Error Correcting Code

Qubits now have a very short "shelf-life," which is one of the main issues preventing physical implementations of quantum computers [1]. Qubits in superposition often have lives on the order of microseconds before they "break"[1], and their state changes unexpectedly, disrupting your computation. This scheme contrasts with classical bits on hard drives or CDs, which persist for years. Because a single encounter with a stray particle or photon might change their state [15, 4], they need to be exceptionally well insulated from the rest of the environment. The circuit will give absurd results when this environment-driven error occurs; it is the same as having a traditional bit on a hard drive sector that can no longer be read or written correctly, resulting in corrupted and meaningless data [17].

To create quantum error-correcting codes to shield quantum states from the effects of noise. It takes new concepts to account for some significant discrepancies between classical and quantum information to implement such quantum error-correcting codes. In particular, it appears that we must overcome three pretty significant challenges:

No cloning: One can attempt to apply the repetition code in quantum mechanics by replicating the quantum state three times or more. The no-cloning theorem forbids this. The three quantum states emitted from the channel cannot be measured or compared, even if cloning were possible [3].

Errors are continuous: A single qubit may experience a continuum of various errors. It would require infinite precision and, thus, unlimited resources to identify which error happened and fix it [3].

Measurement destroys quantum information: Quantum information cannot be measured. Hence, the decoding method is chosen in conventional error correction after observing the channel's output. In quantum physics, observation typically destroys the observed quantum state and renders recovery impossible [3].

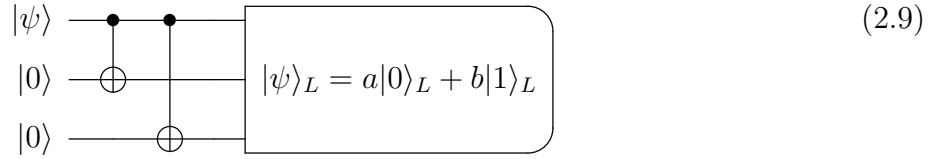
However, nothing can live in an ideal, isolated state completely free from its surroundings. Modern quantum computers effectively compete with time to complete practical computations before the qubits fail [16]. Scientists use various methods to increase this time as much as possible. Most of these use hardware [1], but one method makes use of the software. This method uses error correction codes by tying up a single qubit with many spare qubits so that they are all in the same state simultaneously. The error correction algorithm can use the other qubits to "repair" a qubit if it experiences an error brought on by the environment [16, 17].

### 2.4.1 Quantum Error Correcting Code for Three Qubits

Let us say we send qubits through a channel that flips them with probability  $p$  and keeps them unchanged with probability  $1 - p$ . In other words, the state  $|\psi\rangle$  is changed to the state

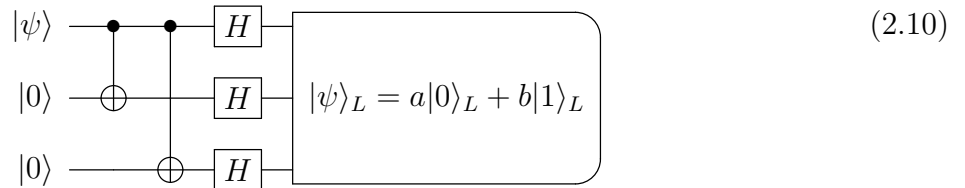
$X|\psi\rangle$  with probability  $p$ , where  $X$  is the standard Pauli  $\sigma_x$  operator or bit-flip operator. We now describe the bit-flip code, which can be used to shield qubits from the effects of noise from this channel, known as the bit flip channel.

Encode the single qubit state  $|\psi\rangle = a|0\rangle + b|1\rangle$  in three qubits as  $a|000\rangle + b|111\rangle$ . The terms  $|000\rangle$  and  $|111\rangle$  can be written as  $|0\rangle_L$  and  $|1\rangle_L$  respectively, this notation indicates that these are the logical  $|0\rangle$  and logical  $|1\rangle$  states, not the physical zero and one states. Encoding circuit for the three qubit bit flip code [16, 17]:



Then 6 exchange interaction gate steps and 6 single-qubit rotation gate steps are required to generate the "Quantum Error-Correcting Code" (QECC) [18] for the 3-qubit bit-flip error.

The phase flip error model for a single qubit is a more intriguing noisy quantum channel. In this mistake model, the qubit is left alone with probability  $1 - p$ , and the relative phase of the  $|0\rangle$  and  $|1\rangle$  states is flipped with probability  $p$ . Phase flip  $Z : |x\rangle \rightarrow (-1)^x|x\rangle$ . The phase flip operator  $Z$  is applied to the qubit, and the state  $a|0\rangle + b|1\rangle$  is converted to the form  $a|0\rangle - b|1\rangle$  under the phase flip. Because classical channels lack the attribute comparable to phase, there is no classical counterpart to the phase flip channel. There is, however, a simple technique to convert the phase flip channel to a bit flip channel[3].



For this code, the  $|0\rangle_L$  and  $|1\rangle_L$  are represented as  $|+++ \rangle$  and  $|--- \rangle$ , respectively, where these are  $|+\rangle = \frac{|0\rangle+|1\rangle}{\sqrt{2}}$  and  $|-\rangle = \frac{|0\rangle-|1\rangle}{\sqrt{2}}$ .

To defend a genuine qubit against these types of mistakes or a combination of these using these codes, the Peter Shor's 9-qubit code code must be employed [18, 21], which is



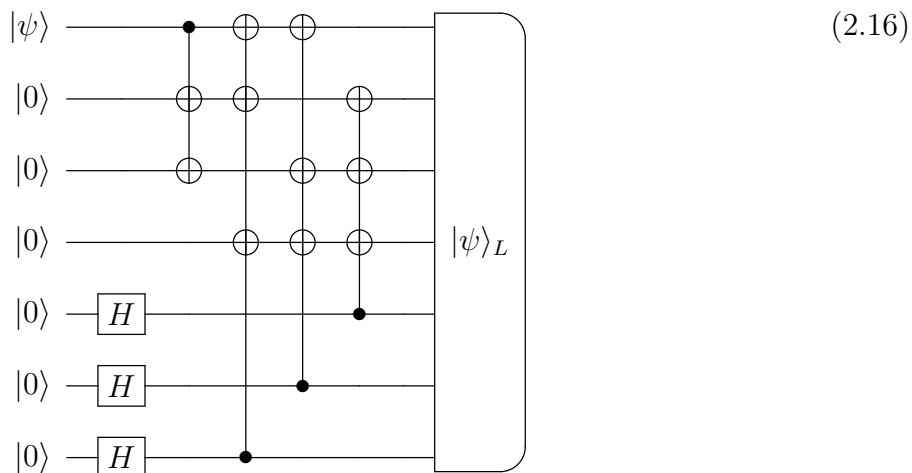
### 2.4.3 Quantum Error Correcting Code for Seven Qubits

In 1996 Andrew Steane improved upon Peter Shor’s 9-qubit code with a 7-qubit code [23]. ”Steane’s code is actually based on a classical error correction code called a Hamming code; essentially it’s the quantum equivalent of it.”[16] The encoding step in the 7-qubit code involves mapping each logical qubit to encoded form according to [21, 23]:

$$|0\rangle_L = \frac{1}{2\sqrt{2}}(|0000000\rangle + |1010101\rangle + |0110011\rangle + |1100110\rangle + |0001111\rangle + |1011010\rangle + |0111100\rangle + |1101001\rangle) \quad (2.14)$$

$$|1\rangle_L = \frac{1}{2\sqrt{2}}(|1111111\rangle + |0101010\rangle + |1001100\rangle + |0011001\rangle + |1110000\rangle + |0100101\rangle + |1000011\rangle + |0010110\rangle) \quad (2.15)$$

Encoding circuit for seven-qubit QECC[21, 23]:



Once in this form the encoded data is protected against a single error in any qubit amongst any of the seven qubits. A total of 99 steps are required, comprising 66 steps for the exchange gate, including 44 steps for the SWAPs and 33 steps for the single-qubit rotation.

# Chapter 3

## Spin Bus

In Chapter 2, the conventional linear array of qubits method to create quantum circuits was explained, this method is through exchange interactions between pairs of neighboring qubits. This chapter demonstrates how to build quantum circuits using a spin-bus multi-qubit gate design that is equally efficient for interactions between neighboring qubits and more efficient for interactions between separate qubits.

### 3.1 Spin Bus Architecture

Because of their long decoherence times and propensity for scalable gating approaches, spin qubits in quantum dots are considered leading possibilities for quantum computation. The exchange coupling is a prominent type of interaction between spins that has long been thought to be critical for quantum computing in quantum dots. In various qubit schemes, architectures that use an intermediary bus to support long-distance interactions between remote qubits have been examined. There are semiconductor device proposals [24]. The bus itself is made up of individual electron spins linked together by strong, static exchange couplings[24]. External spin qubits are dynamically connected to the bus's interior nodes through electrical gates see Figure 3.1. In the Loss and DiVincenzo qubit system, the main physical requirements for building a spin bus are the same as for standard quantum dots [24].

$$H_b = J_b^* \sum_{i=1}^{N-1} s_i^b \cdot s_{i+1}^b \quad (3.1)$$

The Hamiltonian Equation 3.1 describes spin interactions within the bus [24, 25]. In this case, the constituent spins are affected by the bus spin operators known as  $s_i^b$ , and we assume that the bus size  $N$  is strictly odd. Additionally, we take the internal bus couplings known as  $J_b$  to be uniform.

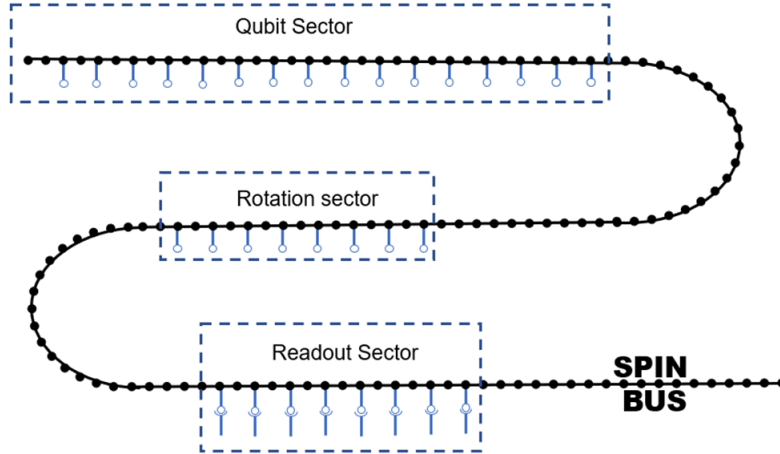


Figure 3.1: "The spin bus is a chain of electronic spins ( $\bullet$ ) with strong, static couplings (heavy lines). External qubits ( $\circ$ ) can be coupled to the bus at any node (light lines). Effective long-range interactions allow for communication between sectors dedicated to rotation, readout or memory, which may benefit from isolation." [25]

The coupling between the  $i$ th qubit and the  $i$ th bus spin is given by  $H_i = J_i(t)s_i^q \cdot s_i^b$ . Restricting the bus to its ground state manifold, we obtain an effective qubit-bus Hamiltonian:

$$H_n = J_q^* \sum_{i=1}^n s_i^q \cdot S \quad (3.2)$$

Where the spin operator  $S$  acts on the spin-1/2 bus manifold. Mathematically, we get that  $J_i^* \simeq J_i/\sqrt{N}$ , where the plus sign is valid for odd bus nodes and the minus sign is valid for even bus nodes. The speed at which the qubit bus operates is thus determined

by the qubit bus coupling strength  $J_i$  and the size of the bus. It has been brought to our attention that the effective couplings  $J_i^*$  switch back and forth between ferromagnetic and antiferromagnetic states. In the following, we will assume that the qubit-bus couplings are uniform ( $J_i = J_q$ , for all  $i$ ) and we will only consider the nodes that are antiferromagnetically linked [25].

The serial mode is the most straightforward method of operation for the bus because it utilizes the bus itself as a qubit proxy. The Heisenberg interaction  $H_i$  generates a *SWAP* gate between the qubit and the bus; The serial gate protocol proceeds as follows [25]:

1. *SWAP* the qubit onto the bus
2. conduct a  $\sqrt{SWAP}$  root-SWAP gate between the bus and the target qubits
3. *SWAP* the bus back onto the original qubit. The optimum end state is a  $\sqrt{SWAP}$  between the qubits, which leaves the bus in its starting state. It should be noted that the starting condition of the bus is unimportant for serial operations.

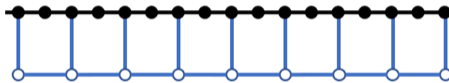


Figure 3.2: Additional local couplings enable parallel interactions, in addition to busmediated interactions [25].

Mark friesen, et al in [25] investigate a SWAP protocol between two qubits on opposite ends of an  $N$ -qubit chain in order to compare the scaling characteristics of the serial bus gate to a traditional linear qubit array. This is accomplished for the typical array using a sequence of  $(2N - 3)$  *SWAP* gates. The total gate time is approximately  $N\pi/J_q$  since several gates with duration  $\pi/J_q$  might be executed in simultaneously. In the case where we have assumed a  $(2N - 1)$ -qubit array with  $N$  antiferromagnetically coupled qubits and  $(N - 1)$  unused ferromagnetically coupled qubits, the appropriate spin-bus protocol only

requires three SWAPs with a total gate time of  $\pi$ . As a result, the bus offers a quadratic speedup for a serial SWAP gate. Local gates, parallel gates, and a small degree of parallel (qubit-qubit) connection are also made possible by this Figure 3.2.

### 3.2 Build Multiqubit Bus Gates

The Hamiltonian  $H_n = J_q^* \sum_{i=1}^n s_i^q \cdot S$  describes simultaneous multiqubit connections to the bus. Except for its multiplicity of couplings, the bus functions like an ordinary qubit when constrained to its working manifold Figure 3.3. We assume here that the effective coupling constants  $J_q^*$  are same for all qubits, while removing this constraint allows for a more diverse collection of multiqubit gates[24, 25].  $U(t) = e^{-iH_n t}$  denotes the unitary evolution operator for the qubit-bus system. Although  $U(t)$  contains offdiagonal terms that entangle the qubits with the bus, with a real bus gate, these terms should vanish. We therefore seek special evolution periods  $t = \tau$  for which bus decoupling occurs [25].

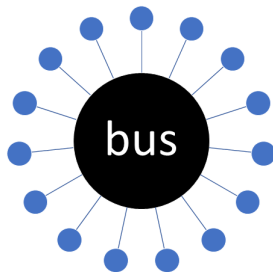


Figure 3.3: Within the ground state manifold, the bus acts as a simple spin-1/2 qubit, except for its plurality of qubit couplings.

Friesen, et al [25] shows how to compute the unitary matrix for the non-trivial case of  $n$  odd. In the angular momentum basis,  $U(t)$  is block diagonal with blocks of size  $1 \times 1$  and

$2 \times 2$ . there exists a time for which all the  $2 \times 2$  blocks are simultaneously diagonal.

$$\hat{U}(t^*) = \mathbb{I}_B \otimes \mathbb{U}_2 \quad t^* = \frac{4\pi}{3J} \quad \text{for } N_q = 2 \quad (3.3)$$

$$\hat{U}(t^*) = \mathbb{I}_B \otimes \mathbb{U}_{N_q} \quad t^* = \frac{2\pi}{J} \quad \text{for } N_q = \text{odd} \quad (3.4)$$

$$\hat{U}(t^*) = \mathbb{I}_B \otimes \mathbb{I}_{N_q} \quad t^* = \frac{4\pi}{J} \quad \text{for } N_q = \text{even}(\neq 2) \quad (3.5)$$

With the exception of the instance  $n = 2$ , we discover that  $U(\tau) = 1$ . We may reorder the basis so that  $U(\tau) = \text{diag}(U_n, U_n) = Id_b \otimes U_n$  since the multiplicity of each diagonal element in  $U(\tau)$  is even. This is an amazing result: the  $U(\tau)$  gate's operation is to restore the bus to its original state while performing a non-trivial mutation  $U_n$  on the qubits. Although  $U(t)$  contains offdiagonal terms that entangle the qubits with the bus, for a real bus gate, these terms should vanish. Is a multi-qubit entangling gate.

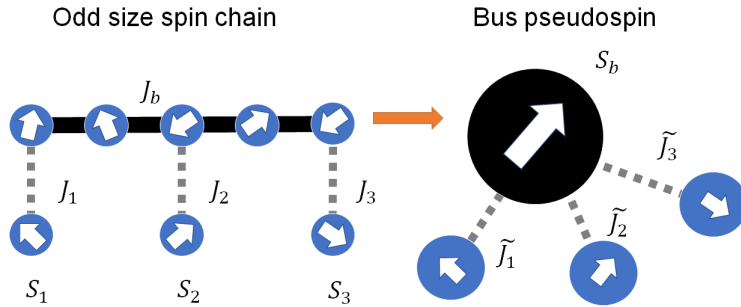


Figure 3.4: With at special times, the unitary operator becomes the bus gates angles only the qubits, not the bus pseudospin

Some examples of multiqubit matrices computed for  $n=2$  and  $n=3$ :

$$U_2 = - \begin{pmatrix} \frac{1}{2}(1 + i\sqrt{3}) & 0 & 0 & 0 \\ 0 & \frac{1}{4}(-1 + i\sqrt{3}) & \frac{1}{4}(1 + i\sqrt{3}) & 0 \\ 0 & \frac{1}{4}(1 + i\sqrt{3}) & \frac{1}{4}(1 - i\sqrt{3}) & 0 \\ 0 & 0 & 0 & \frac{1}{2}(1 + i\sqrt{3}) \end{pmatrix} \quad (3.6)$$

$$U_3 = i \begin{pmatrix} 1 & 0 & 0 & 0 & 0 & 0 & 0 & 0 \\ 0 & -1/3 & 2/3 & 0 & 2/3 & 0 & 0 & 0 \\ 0 & 2/3 & -1/3 & 0 & 2/3 & 0 & 0 & 0 \\ 0 & 0 & 0 & -1/3 & 0 & 2/3 & 2/3 & 0 \\ 0 & 2/3 & 2/3 & 0 & -1/3 & 0 & 0 & 0 \\ 0 & 0 & 0 & 2/3 & 0 & -1/3 & 2/3 & 0 \\ 0 & 0 & 0 & 2/3 & 0 & 2/3 & -1/3 & 0 \\ 0 & 0 & 0 & 0 & 0 & 0 & 0 & 1 \end{pmatrix} \quad (3.7)$$

The 5-qubit and 7-qubit spin bus gate matrices will be utilized in subsequent computations, but they are too huge to write explicitly in the document because they are  $32 \times 32$  and  $64 \times 64$  arrays, respectively.

# Chapter 4

## Optimize Quantum Circuits Using Spin Bus Multiqubit Gate

The "spin bus multiqubit gates" circuits consist of individual qubit operations interspersed between multiqubit operations. The aim is to use the least number of operations possible, that is, to minimize the number of multiqubit gates and the number of single qubit operations. The values of the multiqubit gates are fixed so what is sought are the most optimal parameters in which the fewest number of operations are used.

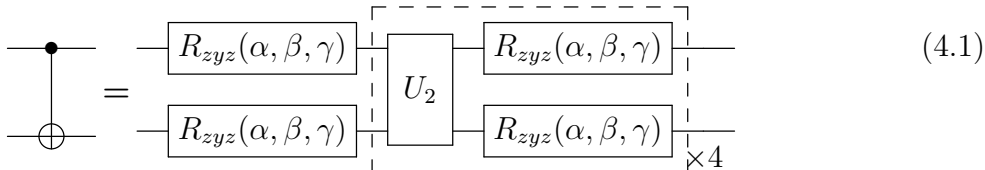
### 4.1 Optimization of Quantum Circuits Using Spin Bus

The process for building quantum circuits using spin qubits and multiqubit gates:

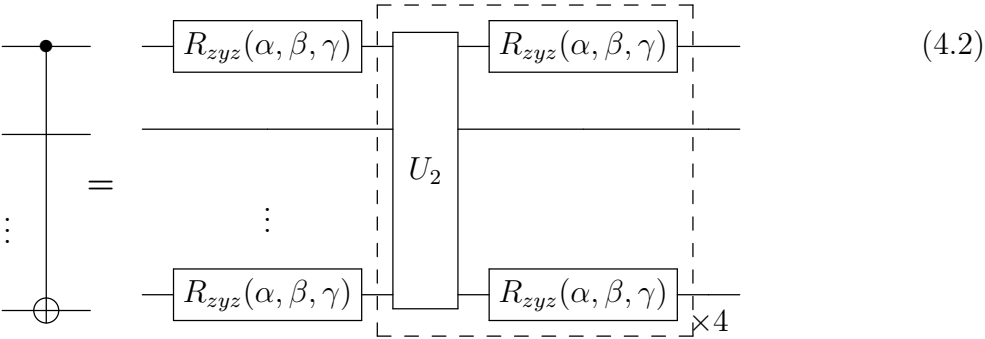
1. To build the circuits, begin with gates for a single qubit for each qubit; any gate of a single qubit can be decomposed as three rotations of angles of two orthogonal axes, as shown in Theorem 1. One qubit unitary gate can be represented by rotational gates  $R_{zyz}(\alpha, \beta, \gamma) = R_z(\alpha)R_y(\beta)R_z(\gamma)$ , where each door is determined by three angular parameters.
2. Multi-qubit gates are next applied to the qubits to form entangled states, which are represented as unitary Matrices, followed by single-qubit gates as in step 1. This procedure is repeated until an acceptable solution is found.
3. Finally, a global phase gate is added to the circuit.

The function  $f(x_i) = |\Psi(x_i) - \Psi_{target}|$  is used to optimize the angular parameters  $x_i$  of the gates of a single qubit, attempting to approximate the result as closely as possible ( $f(x_i) = 0$ ), using an evolutionary differential algorithm and manually modifying the number of multiqubit gates and the number of necessary parameters. The circuit was written in Julia and utilizes the LinearAlgebra packages for matrix representation of quantum logic gates and matrix and vector multiplication, as well as the free-to-use BlackboxOptim package developed by Robert Feldt [26].

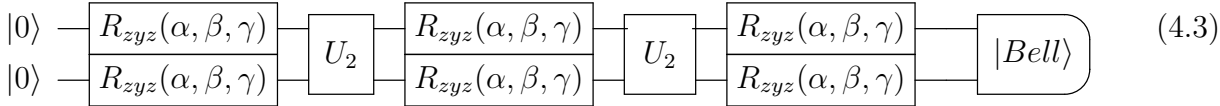
Here some important results of optimization of quantum circuits using spin bus gates. CNOT gate for 1 qubit distance is built using 18 angular parameters and 4 multi-qubit gates:



CNOT gate for n qubit distance gate is built using 18 angular parameters and 4 multi-qubit gates, the requirements are similar to those of the previous circuit, but arranged like this:



The Bell state was built utilizing two multi-qubit  $U_2$  gates and 18 angular parameters that were optimized:



The GHZ state required only a multiqubit gate for three U3 qubits and the optimization of 18 angular parameters:

$$\begin{array}{c}
 |0\rangle \\
 |0\rangle \\
 |0\rangle
 \end{array}
 \begin{array}{c}
 \boxed{R_{zyz}(\alpha, \beta, \gamma)} \\
 \boxed{R_{zyz}(\alpha, \beta, \gamma)} \\
 \boxed{R_{zyz}(\alpha, \beta, \gamma)}
 \end{array}
 \begin{array}{c}
 \boxed{U_3} \\
 \\
 \\
 \end{array}
 \begin{array}{c}
 \boxed{R_{zyz}(\alpha, \beta, \gamma)} \\
 \boxed{R_{zyz}(\alpha, \beta, \gamma)} \\
 \boxed{R_{zyz}(\alpha, \beta, \gamma)}
 \end{array}
 \begin{array}{c}
 \boxed{|GHZ\rangle} \\
 \\
 \\
 \end{array}
 \quad (4.4)$$

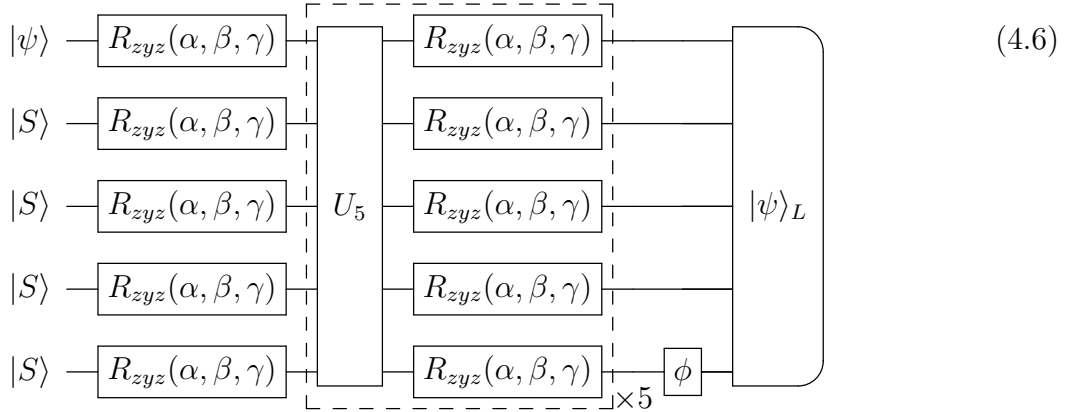
## 4.2 Optimization of Error Correcting Codes Using Spin Bus Gates

We sowed the importance of the quantum error-correcting codes in Chapter 2, and that is why we believe generating these circuits more efficiently is critical. We begin with entangled states between the qubits that will safeguard the target qubit  $|Bell\rangle = |SS\rangle$ , while building quantum error-correcting codes with multiqubit gates. 5 multiqubit gates, 39 angular parameters, and 1 extra parameter for the phase logic gate that reflects were used to optimize the quantum error-correcting code for bit-flip error for 3 qubits. The optimization goal was to achieve a the terms  $|000\rangle$  and  $|111\rangle$  can be written as  $|0\rangle_L$  and  $|1\rangle_L$ .

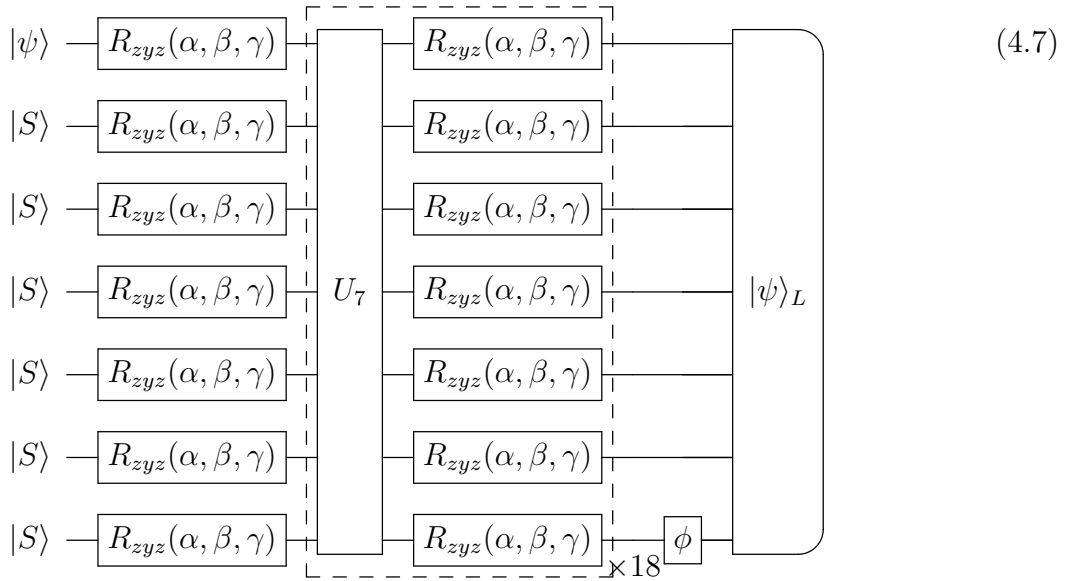
$$\begin{array}{c}
 |\psi\rangle \\
 |S\rangle \\
 |S\rangle
 \end{array}
 \begin{array}{c}
 \boxed{R_{zyz}(\alpha, \beta, \gamma)} \\
 \boxed{R_{zyz}(\alpha, \beta, \gamma)} \\
 \boxed{R_{zyz}(\alpha, \beta, \gamma)}
 \end{array}
 \begin{array}{c}
 \boxed{U_3} \\
 \\
 \\
 \end{array}
 \begin{array}{c}
 \boxed{R_{zyz}(\alpha, \beta, \gamma)} \\
 \boxed{R_{zyz}(\alpha, \beta, \gamma)} \\
 \boxed{R_{zyz}(\alpha, \beta, \gamma)}
 \end{array}
 \begin{array}{c}
 \boxed{\phi} \\
 \\
 \\
 \end{array}
 \begin{array}{c}
 \boxed{|\psi\rangle_L} \\
 \\
 \\
 \end{array}
 \quad (4.5)$$

Five 5-qubit multiqubit gates, 90 angular parameters, and one extra parameter for the phase logic gate that reflects the global phase were used to optimize the quantum error-correcting code for five qubits. The goal of the optimization was to achieve a logical state

similar to that of Equations 2.11 and 2.12:



The quantum error-correcting code for 7 qubits was optimized with 18 multiqubit gates of 7 qubits, 99 angular parameters, and one extra parameter for the phase logic gate that represents the global phase. When developing optimization, the goal was to get to a logical state like equations 2.14 and 2.15:



### 4.3 Comparison

These tables compare the steps required in specific circuits to obtain the required target states. The number of exchange interaction gates (E.I.G.) and the number of spin bus gates (S.B.G.) needed for each circuit with the same target state are compared. And mainly, the

total number of steps necessary to build these circuits is also compared using these different multiqubit gates.

Table 4.1: Comparison of the number of multiqubit gates and number of total steps necessary for the construction of the CNOT gate with 1,2,4 and n qubits of distance.

CNOT				
	Number of		Total steps with	
Distance in qubits	E.I.G.	S.B.G.	E.I.G.	S.B.G.
1	2	4	5	5
2	4	4	7	5
4	8	4	11	5
n	2n	4	2n+3	5

Table 4.1 shows how the number of steps to build a CNOT gate between two qubits increases with the number of qubits of distance using E.I.G. While the number of steps remains constant using S.B.G.

Table 4.2: Comparison of number of multiqubit gates and number of total steps needed to create circuits to obtain entangled states between qubits.

Entangled states				
	Number of		Total steps with	
State	E.I.G.	S.B.G.	E.I.G.	S.B.G.
$ Bell\rangle$	2	2	6	5
$ GHZ\rangle$	6	2	12	3

The most used states for entanglement between qubits are the Bell's state and the GHZ

state for two and three qubits, respectively. It is important to note that using the S.B.G., precisely the same states can be obtained with and retain the same level of entanglement, And they can be built almost as efficiently using S.B.G.

Table 4.3: Comparison of number of multiqubit gates and number of total steps needed to create QECC for 3,5 and 7 qubits.

QECC	3-qubits (bit-flip)	5-qubits	7-qubits
E.I.G.	6	28	66
Total steps with E.I.G.	12	52	99
S.B.G.	7	9	18
Total steps with S.B.G.	14	17	37

QECCs are presently commonly utilized to defend against qubit errors. Table 4.3 indicates that utilizing S.B.G. to build a circuit is substantially more efficient since the total number of steps required is decreased from 52 to 17 for 5-qubit QECC and from 99 to 37 for 7-qubit error-correcting. These comparisons show that employing S.B.G. results in substantially more efficient circuits for qubits. Because it retains the same efficiency for close qubits while being considerably more efficient for distant qubits interactions.

# Chapter 5

## Conclusion

Because there is only a limited supply of physical qubits now accessible, and because it is challenging to produce new qubits and carry out operations with them, it is essential to develop faster and more effective techniques for computations in quantum computers. The exchange interaction method is often inferior to the spin bus architecture in terms of the quality of the entanglement operations that it can perform.

The realization of a comparison between two different methods of designing quantum error correction codes was noteworthy. The first was the decomposition of theoretical circuits into operations that appear in real devices such as SWAP gates, SWAP Root as exchange operations, and the rotations of Rzyz angles for the operations of a single qubit, while the second was obtaining optimized data that can be used for a real quantum circuit of multiqubit spin bus a. The spin bus gate is utilized for entangled qubit operations, while the Rzyz rotations are employed for single qubit operations.

The spin bus architecture provides a far better strategy for long-range qubit interactions. As can be observed in the Tables in 4.1, 4.2 and 4.3 the number of steps required to conduct significant multiqubit operations such as quantum error-correcting are significantly reduced when employing spin bus multiqubit gates. This results in a substantial increase in efficiency. The overall number of operations required is significantly fewer, particularly as the number of qubits in the system grows.

# References

- [1] Eriksson, M., Coppersmith, S. & Lagally, M. Semiconductor quantum dot qubits. *MRS Bulletin*. **38**, 794-801 (2013,10)
- [2] Kloeffel, C. & Loss, D. Prospects for spin-based quantum computing in quantum dots. *Annual Review Of Condensed Matter Physics*. **4**, 51-81 (2013,4)
- [3] Nielsen, M. & Chuang, I. Quantum Computation and Quantum Information. (Cambridge University Press,2010)
- [4] DiVincenzo, D. & Loss, D. Quantum Computers and Quantum Coherence. (1999,1)
- [5] Swan, M., Santos, R. & Witte, F. Quantum Computing. (WORLD SCIENTIFIC (EUROPE),2020,4)
- [6] Slepoy, A. Quantum gate decomposition algorithms (Sandia National Laboratories (SNL),2006,7), <https://www.osti.gov/servlets/purl/889415/>
- [7] Kaye, P., Laflamme, R. & Mosca, M. An Introduction to Quantum Computing. (Oxford University Press,2006,11)
- [8] Muradian, R. Qubits on the Poincaré (Bloch) Sphere. *Wolfram Demonstrations Project*. (2011,3). <https://wolfram.com/QubitsOnThePoincareBlochSphere/>
- [9] Barenco, A., Bennett, C., Cleve, R., DiVincenzo, D., Margolus, N., Shor, P., Sleator, T., Smolin, J. & Weinfurter, H. Elementary gates for quantum computation. *Physical Review A*. **52**, 3457-3467 (1995,11), <https://link.aps.org/doi/10.1103/PhysRevA.52.3457>
- [10] Krol, A., Sarkar, A., Ashraf, I., Al-Ars, Z. & Bertels, K. Efficient decomposition of unitary matrices in quantum circuit compilers. (2021,1), <http://arxiv.org/abs/2101.02993>

- [11] Williams, C. Explorations in Quantum Computing. (Springer London,2011), <http://link.springer.com/10.1007/978-1-84628-887-6>
- [12] Pittenger, A. An Introduction to Quantum Computing Algorithms. (Birkhäuser Boston,2000)
- [13] Shende, V., Markov, I. & Bullock, S. Minimal Universal Two-qubit Quantum Circuits. (2003,8), <http://arxiv.org/abs/quant-ph/0308033>
- [14] Fan, H., Roychowdhury, V. & Szkopek, T. Optimal two-qubit quantum circuits using exchange interactions. (2004,9)
- [15] Loss, D. & DiVincenzo, D. Quantum computation with quantum dots. *Physical Review A*. **57**, 120-126 (1998,1)
- [16] Preston, J. Bit-flip error correction. *Bit-Flip Error Correction - Intro To Quantum Software Development*. (2021,6), <https://stem.mitre.org/quantum/error-correction-codes/bit-flip-error-correction.html>
- [17] Devitt, S., Nemoto, K. & Munro, W. Quantum Error Correction for Beginners. (2009,5), <http://arxiv.org/abs/0905.2794>
- [18] DiVincenzo, D. & Shor, P. Fault-Tolerant Error Correction with Efficient Quantum Codes. *Physical Review Letters*. **77**, 3260-3263 (1996,10)
- [19] Laflamme, R., Miquel, C., Paz, J. & Zurek, W. Perfect Quantum Error Correcting Code. *Physical Review Letters*. **77**, 198-201 (1996,7)
- [20] Knill, E., Laflamme, R., Martinez, R. & Negrevergne, C. Benchmarking Quantum Computers: The Five-Qubit Error Correcting Code. *Physical Review Letters*. **86**, 5811-5814 (2001,6)
- [21] Nakahara, M. & Tetsuo, O. Quantum Computing. (CRC Press,2008,3)

- [22] Touchette, D., Ali, H. & Hilke, M. 5-qubit quantum error correction in a charge qubit quantum computer. (2010,10)
- [23] Steane, A. Error Correcting Codes in Quantum Theory. *Physical Review Letters*. **77**, 793-797 (1996,7)
- [24] Mehring, M. & Mende, J. Spin-bus concept of spin quantum computing. *Physical Review A*. **73**, 052303 (2006,5)
- [25] Friesen, M., Biswas, A., Hu, X. & Lidar, D. Efficient Multiqubit Entanglement via a Spin Bus. *Physical Review Letters*. **98**, 230503 (2007,6)
- [26] Feldt, R. BlackBoxOptim.jl/LICENSE.md at master · blackboxoptim.jl. *GitHub*., <https://github.com/robertfeldt/BlackBoxOptim.jl.md>

# Curriculum Vitae

On September 17, 1995, Miguel G. Rodriguez was born. He is the first son of Miguel Rodriguez and Claudia Ramirez. He graduated in the spring of 2014 from Centro de bachillerato industrial y de servicios No.114 in Ciudad Juarez, Chihuahua, Mexico. Where his interest in science was sparked, and where he competed in science competitions, winning several of them. In the autumn of 2016, he enrolled at the Autonomous University of Juarez City. Where to study mathematics and where he was the best in his class, occasionally receiving accolades for the highest average and decided to concentrate in his terminal field in Physics He will begin his studies at The University of Texas at El Paso's Graduate School in the autumn of 2020. He worked as a Teaching Assistant and Research Assistant while obtaining a master's degree in Physics. He aspires to learn more and to make significant scientific advances that will aid in the comprehension of the universe.